

Ridge Curves and Shape Analysis

J.T. Kent, K.V. Mardia and J.M. West

Department of Statistics

University of Leeds

Leeds, LS2 9JT

United Kingdom

Abstract

Ridge curves are important features in human vision (see Koenderink, 1990, p.295). In this paper we apply a simple algebraic criterion of Porteous (1994) to the problem of finding ridge curves in machine vision. This work provides a simpler approach than other existing methods (see for example, Thirion and Gourdon, 1992, and Hosaka, 1992). To identify ridge curves in practice on surface data it is necessary first to smooth the data, which we do using thin-plate splines and related kriging procedures. After validating our methodology, we illustrate its use on a set of laser range data of the human head.

1 Introduction

Intuitively ridge curves on a surface occur at points where the curvature is changing most rapidly. There is some evidence that the human eye picks out ridge curves when looking at a surface. For example, for the human face the ridge curves seem to correspond to prominent anatomical features. It is claimed that ridge curves “usually appear, along with edges of regression, in line drawings of scenes arising as quick sketches or intended as caricatures”, Cutting et al (1993).

In this paper a simple algebraic criterion is used to define ridge curves. This approach can be contrasted with apparently more complicated existing approaches (see, for example, Thirion and Gourdon, 1992 and Hosaka, 1992). Some detailed comments are given in Section 2 below. Since our ridge criterion depends on third derivatives, it is very sensitive to noise. Therefore, we investigate the use of smoothing a discrete representation of a surface using smoothing thin-plate splines and related kriging predictors.

Koenderink (1990, p.290), points out that ridge curves are significant features of a surface in computer vision. For a thorough mathematical treatment of ridge curves, see Porteous (1994). Ridge curves were plotted by Gordon (1991) as a step towards facial recognition but bilinear interpolation was used among the local neighbours of a pixel to find ridge points rather than the algebraic criterion described below. A subset of ridge curves called the crest lines has been investigated by the research group at INRIA using the implicit function theorem to calculate derivatives of a surface, after first carrying out edge detection on CT and MRI images (see Ayache, 1995 and Guézic, 1995). Kent, Mardia and Rabe (1994) analyse curvatures for 3-D laser scans of the human face.

One of the reasons for looking at ridge curves is that they are “robust” in the sense that as a surface deforms smoothly, so do the ridge curves. In this sense ridge curves are unlike principal curves.

After preliminary validation of our methodology, we apply our method to obtain ridge curves for laser range data of the human face. In particular, it will be shown how ridge curves can be used to identify key features.

2 Mathematical Formulation

A surface in three dimensional space can be represented, at least locally, by the equation

$$z = f(x, y).$$

Before defining ridge curves it is necessary to set up two preliminary concepts, the tangent plane at a point on the surface and the principal directions in this tangent plane. See e.g. Porteous (1994) for more details.

The tangent plane at a point (x, y) is spanned by the two vectors

$$\mathbf{u} = \begin{bmatrix} 1 \\ 0 \\ f_x \end{bmatrix}, \mathbf{v} = \begin{bmatrix} 0 \\ 1 \\ f_y \end{bmatrix}.$$

Here $f_x = \partial f / \partial x$ etc. Thus, a two dimensional vector $p = (p_1, p_2)$ defines a vector in the tangent space, $p_1 \mathbf{u} + p_2 \mathbf{v}$.

Each direction $p_1 \mathbf{u} + p_2 \mathbf{v}$ in the tangent plane gives rise to a plane curve called a normal curve. This is obtained by intersecting the surface with the plane spanned by the normal (given by $\mathbf{u} \times \mathbf{v}$) to the

surface and the direction $p_1\mathbf{u} + p_2\mathbf{v}$. The curvature of the normal curve at (x, y) depends on the direction of p . The directions for which this curvature is extremal are called principal directions and the corresponding curvatures are called principal curvatures. The principal directions and curvatures can be found as the (right) eigenvectors and eigenvalues, $\kappa_1 \geq \kappa_2$, say, of the matrix $A^{-1}B$, where

$$A = \begin{bmatrix} 1 + f_x^2 & f_x f_y \\ f_x f_y & 1 + f_y^2 \end{bmatrix}$$

is the matrix of the first fundamental form, and

$$B = (1 + f_x^2 + f_y^2)^{-\frac{1}{2}} \begin{bmatrix} f_{xx} & f_{xy} \\ f_{xy} & f_{yy} \end{bmatrix}$$

is the matrix of the second fundamental form. Points at which the two eigenvalues are equal ($\kappa_1 = \kappa_2$) are known as umbilic points. At such points the principal axes are no longer uniquely defined, which causes difficulties. For the most part umbilic points are excluded from the discussion below.

Principal curves on the surface are curves whose tangent directions always point in a principal direction. There are two principal curves passing through each non-umbilic point, corresponding to the larger and smaller eigenvalues of $A^{-1}B$, respectively. Thus there are two families of principal curves on the surface.

Along a principal curve, the value of the corresponding principal curvature changes and at certain points has local extrema. These points are called ridge points and the set of all such points forms a collection of curves called ridge curves. There are two sets of curves, one for the larger and one for the smaller eigenvalue of $A^{-1}B$. Further, each ridge point can be classified according to whether the curvature is maximal or minimal. Porteous (1994, p.187) gives an algebraic condition for a point to be a ridge point, equivalent to the following for a surface given by $z = f(x, y)$. If $p = (p_1, p_2)$ is a principal direction with corresponding non-zero principal curvature κ_p (so p is an eigenvector of $A^{-1}B$ with corresponding eigenvalue κ_p) at the point (x, y) , then (x, y) is a ridge point if and only if

$$\begin{aligned} R(x, y) &= (p_1^3 f_{xxx} + 3p_1^2 p_2 f_{xxy} + 3p_1 p_2^2 f_{xyy} + p_2^3 f_{yyy}) \\ &\quad - 3(1 + f_x^2 + f_y^2)^{\frac{1}{2}} (p_1^2 f_{xx} + 2p_1 p_2 f_{xy} + p_2^2 f_{yy}) (p_1 f_x + p_2 f_y) \kappa_p = 0. \end{aligned} \tag{1}$$

This equation defines a set of curves in the (x, y) plane, which project up to ridge curves on the surface.

Hosaka (1992, p.97, eq.7.28) derives an equation for the loci of extrema of principal curvatures. We note here that this equation determines the extrema of *either* principal curvature along a principal curve rather than just the corresponding principal curvature. Thus ridge curves form only part of the set of points detected by Hosaka's equation. The remaining curves, where the other principal curvature has an extremum along a line of curvature, have been called sub-parabolic curves (Porteous, 1990, p.224). In practice the extremum curvature points are determined numerically while tracing each line of curvature making a complicated procedure.

Researchers at INRIA have obtained crest lines. These are the loci of points whose maximal (in absolute value) principal curvature is a local extremum along a corresponding principal curve. They work with implicitly defined surfaces and seek extrema of curvature directly, with seemingly more complicated algebra than that given by Equation (1) (see e.g. Thirion and Gourdon, 1992, 1993). However, an advantage of an implicit representation of a surface is that a global representation of the surface can be obtained rather than just a local representation.

3 Smoothing

Laser range data can be represented as a series of heights over a grid of pixels. In order to use the above equations from differential geometry, it is necessary to fit a surface to the pixel data, either interpolating or smoothing it. Because of the sensitivity of third derivatives to small scale variations in the data, smoothing of the data is essential before calculating ridge curves.

The method of smooog we have employed is kriging. This is based on the assumption that there is a stochastic process $Z(x, y)$ which follows a stationary (or intrinsic) random field model, with known covariance function (or conditionally positive definite covariance function) $\sigma(h)$, where $h \in \mathbb{R}^2$ denotes the lag, and a specified vector space of drift or trend functions. Typically the drift space is given by polynomials in h up to a specified order.

We observe data

$$W_i = Z(x_i, y_i) + \epsilon_i \quad , \quad \epsilon_i \sim N(0, \lambda), i = 1, \dots, n,$$

where the ϵ_i are noise terms independent of one another. The objective is to estimate $Z(x, y)$ on the basis of the observations W_i , $i = 1, \dots, n$. The predicted surface $\hat{Z}(x, y)$, say, is known as the kriging surface and details of its computation can be found for example in Mardia et al (1996). The derivatives of the kriging surface $\hat{Z}(x, y)$ are used to compute ridge curves.

The known parameter $\lambda \geq 0$ represents the amount of smoothing. If $\lambda = 0$, the fitted surface is an interpolating surface matching the data points exactly. On the other hand, as $\lambda \rightarrow \infty$ the fitted surface tends to the least squares regression surface of the data. The use of the parameter λ is similar to a multi-resolution analysis in which we try to pick out features in the data at different scales. In this case we are looking for a single scale which seems to give the most reliable indication of anatomically significant ridge curves. One set of choices for $\sigma(h)$ (based on intrinsic processes) depending on a parameter $\alpha > 0$ is given by

$$\sigma(h) = (-1)^{[\alpha]+1} \|h\|^{2\alpha}, \alpha > 0, \alpha \text{ not an integer},$$

$$\sigma(h) = (-1)^{\alpha+1} \|h\|^{2\alpha} \log \|h\|, \alpha > 0, \alpha \text{ an integer},$$

with the drift space consisting of polynomials in h of degree $\leq [\alpha]$. A motivation for this particular covariance structure is that the resulting processes are self-similar: for noninteger α , dilating h by $c > 0$ yields a re-scaled covariance function, $\sigma(ch) = c^{2\alpha}\sigma(h)$; for integer α , an analogous result holds. For $\alpha = 1$ the kriging surface can be identified with a thin-plate smoothing spline. Also, as α increases, the kriging surface becomes smoother; for $2\alpha > p$ the surface is p -times continuously differentiable. These kriging surfaces can also be constructed in terms of radial basis functions.

4 Implementation

We use a zero-tracing algorithm to plot ridge curves on a surface. The surface is first triangulated, e.g. by placing a fine square grid over the (x, y) plane and by dividing each square into two triangles. In the applications a 100×100 grid was used.

We track each curve as it crosses the edges of the triangles. The process is complicated by the presence of umbilic points. Around such points it is impossible to find a continuous, non-vanishing oriented principal direction field (see Morris, 1996). Inspection of the ridge criterion, Equation (1) shows that if $p = (p_1, p_2)$ is replaced by $-p = (-p_1, -p_2)$, the criterion changes sign. Thus to find a zero of the ridge criterion along a line segment we must check that the principal directions at each end, p and q , say, are coherently oriented. If the inner product $\langle p, q \rangle$ of p and q is close to $+1$, then the two principal directions have the same orientation and we can test for zeros by seeking a sign change of $R(x, y)$ along the line segment. If the inner product of p and q is close to -1 , then there will be a zero if the sign of $R(x, y)$ is the same at either end of the line segment. Thus in practice we conclude that a ridge curve passes through a line segment with end points (x_1, y_1) and (x_2, y_2) and respective principal directions p and q if

$$R(x_1, y_1)R(x_2, y_2) \langle p, q \rangle < 0.$$

Linear interpolation of $R(x, y)$ is used to determine where the zero of $R(x, y)$ lies.

We find umbilic points using a method of Morris (1996). Either one or three ridges pass through an umbilic point, and at such points each curve changes from being an extremum of one curvature to being an extremum of the other curvature (Porteous, 1994, p.202). Thus either one or three zeros of the ridge condition (for one of the curvatures) around the edges of a triangle indicates the presence of an umbilic point.

Some initial validation of the ridge tracing program has been given using the following example without noise. For a surface of revolution given by $(g(u), h(u) \cos v, h(u) \sin v)$ every meridian (profile curve) is a ridge curve. The only other ridge curves on the surface are those (circular) parallels corresponding to vertices (turning points of curvature) of the generating curve $(g(u), h(u))$. The program was adapted to track only one set of ridge curves and successfully detected the ridge curve on the surface of revolution generated by the plane curve $(u, u^2 + u^4 + 3)$ which has an isolated vertex when $u = 0$. See Fig.1 and Fig.2 for the result. The slight perturbations in the curve are due to the use of linear interpolation to find the zeroes of the ridge criterion.

5 Applications

In this section examples will be given using the intrinsic random field with $\sigma(h) = -|h|^5$ and quadratic drift, with different choices of λ on a laser scan of a human face to illustrate the effectiveness of our procedure. The kriging surface was fitted using 200 points approximately equally spaced over the front of the face.

In Figs.3,4,5 and 6 the white and black curves correspond to the minimal and maximal curvatures respectively. Notice that ridge curves can change colour at umbilic points. For a description of the configurations of ridge curves that can occur at umbilic points, see Porteous (1994). Fig.3 gives the ridge curves for $\lambda = 0$. This picture is too cluttered and too affected by small-scale features on the surface for much structure to be visible. Fig.4 shows a smoother version with $\lambda = 0.01$; the noise is much reduced. For $\lambda = 1,000$ Fig.5 shows just two main ridges of the face remaining, with all the detail smoothed away.

Thus Fig.4 provides a good compromise. The main features depicted in Fig.4 remain stable over several orders of magnitude for λ , though the detailed structure can vary quite substantially. In Fig.4 the vertical white curve corresponds to the midline of the nose, and the outer black curve picks out the outline of the nose. The “horizontal” curve that changes colour twice goes across the top of the nostril part of the nose. The black curve below the nose represents the upper lip of the mouth. Other ridge curves follow features around the cheeks and eyes. These features are clearly seen in Fig.6 which gives a perspective view of Fig.4 with its underlying nose surface being replaced by that in Fig.3.

One pleasing aspect of Fig.4 is the level of symmetry of the ridge curves between the left and right sides of the face. A requirement of symmetry was not imposed on the algorithm or on the choice of landmarks. Thus the symmetry of the output provides evidence that our estimated ridge curves represent meaningful features on the surface.

For the nose laser scan, we have experimented with other choices of $\sigma(h)$ such as $\exp(-c|h|^2)$. The results are somewhat similar in essence but the smoothing does not remove clutter as effectively.

6 Discussion

We have given one practical example from laser range data as well as some validation. The use of Porteous's criterion for a ridge curve is simple from a computational point of view. However, this work is merely a first step in the use of ridge curves to statistically summarize and compare surfaces. Further work is required to assess the replicability of ridge curves, how much "clutter" to remove and the amount of smoothing needed to reliably compute third derivatives. Methods such as cross-validation and scale space ideas (e.g. Lindeberg, 1994) for the automatic selection of λ need to be investigated. As well, a thorough comparison with other methods of smoothing such as moving averages is needed. Future work includes plotting ridge curves for the full face and the skull and using ridge curves for registration and data summary.

Acknowledgements

The authors are grateful to Anne Coombes, Delman Lee, Alf Linney, Richard Morris and Sophia Rabe for helpful discussions and assistance. Three referees provided useful comments. This work is supported by an EPSRC grant under the Complex Stochastic Systems Initiative.

References

- [1] Ayache, N. Medical computer vision, virtual reality and robotics-promising research tracks. *Proceedings BMVC*, 1995, pp.1-25.
- [2] Cutting, C.B., Bookstein, F.L., Haddad, B., Dean, D., Kim, D. A spline-based approach for averaging three-dimensional curves and surfaces. *Mathematical Methods in Medical Imaging II*. Eds. Wilson, J.N., Wilson, D.N., *SPIE Proceedings*, **2035**, 1993, pp.29-44.
- [3] Gordon, G.G. Face Recognition from Depth and Curvature. PhD thesis, Harvard University, 1991.
- [4] Guéziec, A. Surface representation with Deformable Splines: Using Decoupled Variables. *IEEE Computational Science and Engineering*, **2**, 1995, pp.69-80.

- [5] Hosaka, M. *Modeling of Curves and Surfaces in CAD/CAM*. Springer-Verlag, Berlin, 1992.
- [6] Kent, J.T., Mardia, K.V., Rabe, S. Face description from laser range data. *Mathematical Methods in Medical Imaging III*. Eds. Bookstein, F.L., Duncan, J.S., Lange, N., Wilson, D.C., *SPIE Proceedings*, **2229**, 1994, pp.32-45.
- [7] Koenderink, J.J. *Solid Shape*. The MIT Press, Cambridge, Mass, 1990.
- [8] Lindeberg, T. Scale space theory: a basic tool for analysing structures at different scales. *Statistics and Images Vol.2*, ed. K.V. Mardia, Carfax Publishing Co., Abingdon, 1994, pp.225-270.
- [9] Mardia, K.V., Kent, J.T., Goodall, C.R., Little, J.A. Kriging and splines with derivative information. *Biometrika*, 83, 1996, pp.207-221.
- [10] Morris, R.J. The sub-parabolic lines of a surface. *The Mathematics of Surfaces VI*, ed. G. Mullineux, Clarendon Press, Oxford, 1996, pp.79-102.
- [11] Porteous, I.R. *Geometric Differentiation*. Cambridge University Press, Cambridge, 1994.
- [12] Thirion, J-P., Gourdon, A. The 3D marching lines algorithm and its application to crest lines extraction. *Research Report No. 1672*, INRIA, Epidaure, 1992.
- [13] Thirion, J-P., Gourdon, A. The marching lines algorithm: new results and proofs. *Research Report No. 1881-2*, INRIA, Epidaure, 1993.

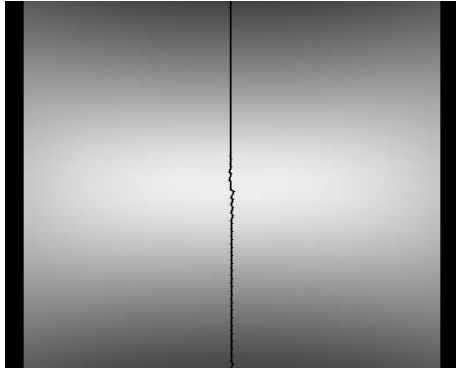


Fig.1: Top view of part of surface of revolution with ridge curve shown.

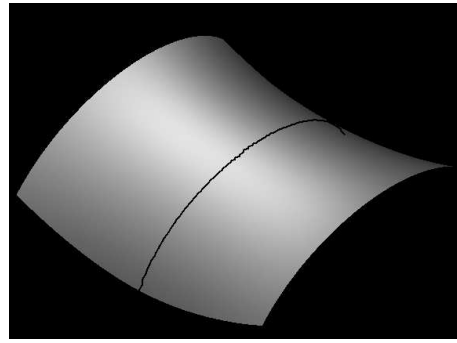


Fig.2: Side view of part of surface of revolution with ridge curve shown.

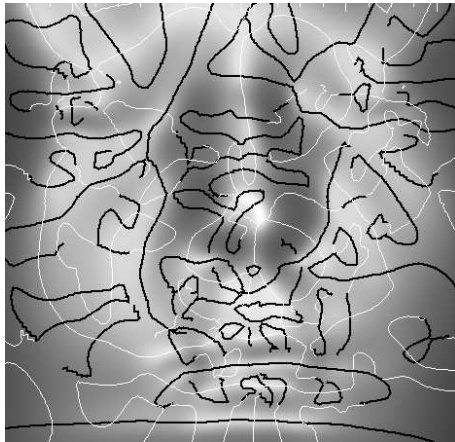


Fig.3: The ridge curves for a face with $\lambda = 0$.

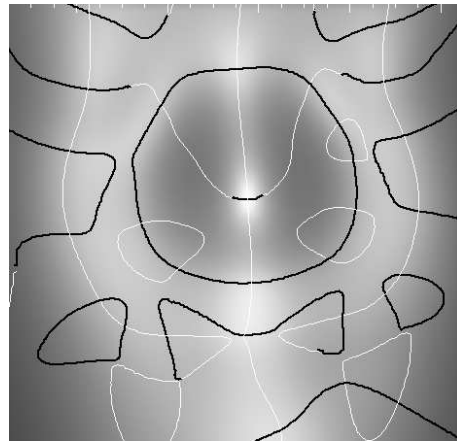


Fig.4: The ridge curves for a face with $\lambda = 0.01$.

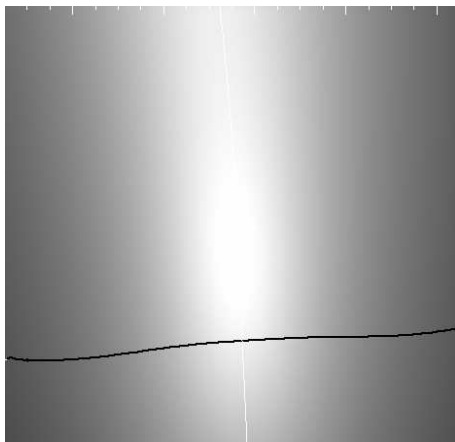


Fig.5: The ridge curves for a face with $\lambda = 100$.

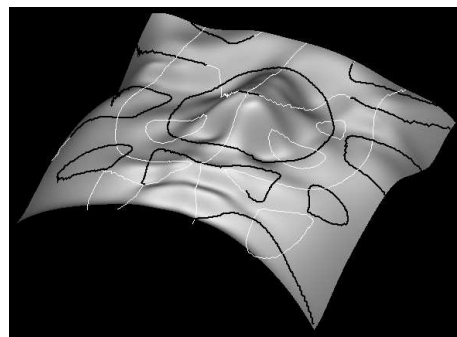


Fig.6: The perspective view of the ridge curves of Fig.4 projected onto the unsmoothed face of Fig.3.